IEEE Access
Multidisciplinary | Rapid Review | Open Access Journal

Received June 14, 2021, accepted July 6, 2021, date of publication July 12, 2021, date of current version July 20, 2021.

Digital Object Identifier 10.1109/ACCESS.2021.3096184

Fuzzy Finite Memory State Estimation for Electro-Hydraulic Active Suspension Systems

HYUN DUCK CHOI[1] **AND SUNG HYUN YOU**[2]
[1]Department of ICT Convergence System Engineering, Chonnam National University, Gwangju 61186, South Korea
[2]Department of Electronics Engineering, Chosun University, Gwangju 61452, South Korea

Corresponding author: Sung Hyun You (you@chosun.ac.kr)

This work has supported in part by the National Research Foundation (NRF) of Korea grant funded by the Korea government (Ministry of Science and ICT) under Grant number NRF-2020R1G1A1101070; in part by the Chonnam National University (Grant number: 2020-1942); and in part by the National Research Foundation (NRF) of Korea grant funded by the Korea government (Ministry of Science and ICT) under Grant number NRF-2020R1G1A1103036.

ABSTRACT This paper presents a novel nonlinear estimator called the fuzzy finite memory (FFM) state estimator for electro-hydraulic active suspension systems, based on fuzzy techniques and finite impulse response. The Takagi-Sugeno fuzzy model is introduced to effectively describe highly nonlinear suspension systems with electro-hydraulic actuator dynamics. Compared with the conventional state estimator, which has an infinite memory structure and requires whole data from the initial to current time, the proposed fuzzy state estimator with a finite memory structure guarantees robustness against external disturbances and modeling uncertainty. The simulation results verify that the developed fuzzy finite memory state estimator is more robust under external disturbances and modeling uncertainties than the existing infinite impulse response nonlinear estimator.

INDEX TERMS Half-vehicle suspension system, state estimation, finite memory structure, electro-hydraulic actuator, nonlinear systems, T-S fuzzy model.

I. INTRODUCTION

Currently, automotive electronics technology is being developed for the safety and comfort of drivers and passengers. Furthermore, the installation rates of vehicle control systems, such as rollover protection systems, adaptive cruise control systems, and electronic stability control (ESC) are increasing worldwide [1]. Among them, active suspension systems that can improve vehicle comfort and steering stability are attracting significant interest from academia and the industry [2], [3]. Vehicle suspensions are classified as passive, semi-active, and active according to the installed elements [4]–[6]. Active suspension is known to be effective in improving ride comfort and driving performance and has significant potential because the actuators that can add or dissipate energy are arranged in parallel with passive components [7], [8].

In practical applications of active suspension systems, the actuator must provide the desired force for control and be suitable for packaging space, power, and bandwidth requirements [9], [10]. Therefore, an appropriate actuator must be selected. Electro-hydraulic actuators are known to be the most suitable for active suspension systems owing to their high power-to-weight ratio and low cost [11], [12]. As a result, numerous studies have been conducted on electro-hydraulic active suspensions in recent years [13]–[15]. However, the highly nonlinear characteristics of the actuators complicate the control design. Most recently, adaptive control of the electro-hydraulic servomechanisms using the extended state observer (ESO) and the output feedback backstepping control of hydraulic actuators, compensating for a delay using the ESO, was developed [39], [40]. Furthermore, considering the interaction between the vehicle suspension systems and the actuator, the implementation of the actuator becomes more difficult in many practical applications [16].

Over the past decades, Takagi-Sugeno (T-S) fuzzy systems have become a popular tools for describing nonlinear systems [17]. The main concept of the T-S fuzzy technique is to approximate a nonlinear system using a fuzzy blending of local dynamics [18], [19]. Therefore, a complex nonlinear system can be expressed as a linear time-varying system through fuzzy membership functions and IF-THEN rules, and the existing linear technology can be successfully applied to stability analysis and control design [20], [21]. Owing to the characteristics of the T–S fuzzy model, which approximates nonlinear systems more accurately than the existing Taylor approximation, several filter design results

The associate editor coordinating the review of this manuscript and approving it for publication was Haibin Sun.

based on the T–S fuzzy model have been presented. A fuzzy state/disturbance observer for integral sliding mode control was designed in [22]. An adaptive sliding-mode observer design was introduced in [23]. Wang *et al.* presented a fuzzy observer for estimating the vehicle roll angle and roll rate [24].

However, most studies on the control design of active suspension systems are related to the state feedback structure. Note that state feedback requires the assumption that all state variables are measurable [25]. However, this is unrealistic in many practical aspects. In terms of cost and complexity, the online measurement of all state information is difficult to implement. Estimating the state through available output measurements is desirable for creating a suitable controller for several applications. Therefore, the estimation of state information is essential for achieving a suitable feedback controller, and many studies have been conducted on the estimation problem. For example, a Luenberger-type state observer was introduced in [27] for nonlinear tracking control of suspension systems. An adaptive Kalman filter for suspension state estimation was presented in [28]. Na *et al.* proposed an active adaptive estimator for vehicle suspensions [29]. In [30], a position tracking controller for a quadrotor was proposed using an ESO technique. However, it should be noted that all aforementioned studies have an infinite impulse response (IIR) structure.

As mentioned before, most state estimators used in actual applications have IIR structures that require all historical input and output data to estimate the current state variable [31], [32]. Owing to the structural characteristics of the IIR estimator, performance degradation or divergence problems can occur when incorrect information or modeling uncertainty occurs [33], [37], [38]. Consequently, finite-memory-based state estimators have received much interest as alternatives to IIR-based state estimation. Many studies have demonstrated that the state estimator based on the finite memory structure is robust against incorrect information and modeling uncertainty compared with the IIR-based state estimator [34]–[36].

Despite being an important topic for feedback control, to the best of our knowledge, only a few papers address the state estimator design problem for active suspension systems. In particular, results on finite-memory state estimators for active suspension systems have not yet been studied in literature; this was the motivation for our study. In this study, for the first time, we investigate a new fuzzy finite-memory state-estimation problem for active suspension systems, including nonlinear electro-hydraulic actuator dynamics. The main contributions and novelty of this study are as follows:

- The fuzzy finite memory state estimator design of active suspension systems with electro-hydraulic actuator is dealt with for the first time.
- By solving the minimum length solution of the cost function, which contains the Frobenius-norm of the fuzzy finite memory estimator gain, the design problem of the proposed estimator for the nonlinear suspension system has been effectively solved.
- The proposed fuzzy finite memory state estimator does not require noise information and uses only recent measurements. In other words, the proposed estimator is robust against uncertainty using a finite memory structure without noise statistics.
- The robustness of the proposed finite memory state estimator against disturbance and model uncertainty are effectively verified under different road conditions via numerical examples.

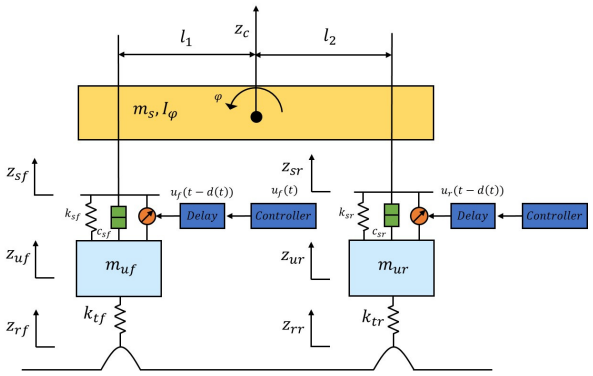

FIGURE 1. 4-DOF suspension model.

The remainder of this paper is organized as follows. In section 2, we present the procedure for obtaining the T-S fuzzy suspension model, including the electro-hydraulic actuator dynamics. The design of the finite memory filter for the T-S fuzzy model is presented in section 3. Section 4 presents the simulation results and discussion. Finally, the conclusions are presented in section 5.

II. NONLINEAR HYDRAULIC SUSPENSION SYSTEM AND ITS APPROXIMATION

The half-vehicle model, which is commonly used for suspension control design, is shown in Figure 1. This 4-degree of freedom(4-DOF) model, owing to the motion in the heave and pitch directions of the sprung mass and the motion in the vertical directions of the unsprung masses, captures more detailed features than the quarter-vehicle model. In this figure, $z_{sf}(t)$ and $z_{sr}(t)$ are the displacements at the front and rear bodies, respectively; $z_{uf}(t)$ and $z_{ur}(t)$ are the displacements at the front and rear unsprung masses, respectively. Furthermore, $z_{rf}(t)$ and $z_{rr}(t)$ are the displacements at the front and rear terrain heights, respectively; $\varphi(t)$ represents the pitch angle of inertia at the center of gravity(CG) points. The pitch moment of inertia about the CG point is represented by I_φ, m_s denotes the mass of the vehicle body, and $z_c(t)$ denotes the displacement of the CG point. The unsprung masses on the front and rear wheels are represented by m_{uf} and m_{ur}, respectively; k_{sf} and k_{sr} represent the stiffness coefficients at the front and rear tires, respectively. The damping coefficients at the front and rear wheels are represented by c_{sf} and c_{sr}, respectively. Finally, $u_f(t)$ and $u_r(t)$ denote the forces at the

TABLE 1. Variable description.

Suspension deflection(front body):	$z_{sf}(t) - z_{uf}(t)$
Suspension deflection(rear body):	$z_{sr}(t) - z_{ur}(t)$
Tire deflection(front body):	$z_{uf}(t) - z_{rf}(t)$
Tire deflection(rear body):	$z_{ur}(t) - z_{rr}(t)$
Vertical velocity(front body):	$\dot{z}_{sf}(t)$
Vertical velocity(rear body):	$\dot{z}_{sr}(t)$
Vertical velocity(front wheel):	$\dot{z}_{uf}(t)$
Vertical velocity(rear wheel):	$\dot{z}_{ur}(t)$

front and rear actuators, respectively. Assuming that $(\varphi(t))$ is negligibly small, we can easily obtain the following equation:

$$z_{sf}(t) = z_c(t) - l_1\varphi(t), \tag{1}$$
$$z_{sr}(t) = z_c(t) + l_2\varphi(t). \tag{2}$$

Placing the origin for the displacement of the CG point and the angular displacement of the vehicle body at static equilibrium and applying Newton's second law, we can express the suspension equation as follows:

$$\begin{aligned}
&m_s\ddot{z}_c(t) + k_{sf}[z_{sf}(t) - z_{uf}(t)] + c_{sf}[\dot{z}_{sf}(t) - \dot{z}_{uf}(t)] \\
&\quad + k_{sr}[z_{sr}(t) - z_{ur}(t)] + c_{sr}[\dot{z}_{sr}(t) - \dot{z}_{ur}(t)] \\
&\quad = u_f(t) + u_r(t), \\
&I_\varphi\ddot{\varphi}(t) - l_1k_{sf}[z_{sf}(t) - z_{uf}(t)] - l_1c_{sf}[\dot{z}_{sf}(t) - \dot{z}_{uf}(t)] \\
&\quad + l_2k_{sr}[z_{sr}(t) - z_{ur}(t)] + l_2c_{sr}[\dot{z}_{sr}(t) - \dot{z}_{ur}(t)] \\
&\quad = -l_1u_f(t) + l_2u_r(t), \\
&m_{uf}\ddot{z}_{uf}(t) - k_{sf}[z_{sf}(t) - z_{uf}(t)] - c_{sf}[\dot{z}_{sf}(t) - \dot{z}_{uf}(t)] \\
&\quad + k_{tf}[z_{uf}(t) - z_{rf}(t)] = -u_f(t), \\
&m_{ur}\ddot{z}_{ur}(t) - k_{sr}[z_{sr}(t) - z_{ur}(t)] - c_{sr}[\dot{z}_{sr}(t) - \dot{z}_{ur}(t)] \\
&\quad + k_{tr}[z_{ur}(t) - z_{rr}(t)] = -u_r(t),
\end{aligned} \tag{3}$$

From (1)–(3), the following can be easily obtained:

$$\begin{aligned}
\ddot{z}_{sf}(t) &= \ddot{z}_c(t) - l_1\ddot{\varphi}(t) \\
&= a_1\{u_f(t - d(t)) - k_{sf}[z_{sf}(t) - z_{uf}(t)] \\
&\quad - c_{sf}[\dot{z}_{sf}(t) - \dot{z}_{uf}(t)]\} + a_2\{u_r(t - d(t)) \\
&\quad - k_{sr}[z_{sr}(t) - z_{ur}(t)] - c_{sr}[\dot{z}_{sr}(t) - \dot{z}_{ur}(t)]\}, \\
\ddot{z}_{sr}(t) &= \ddot{z}_c(t) - l_2\ddot{\varphi}(t) \\
&= a_2\{u_f(t - d(t)) - k_{sf}[z_{sf}(t) - z_{uf}(t)] \\
&\quad - c_{sf}[\dot{z}_{sf}(t) - \dot{z}_{uf}(t)]\} + a_3\{u_r(t - d(t)) \\
&\quad - k_{sr}[z_{sr}(t) - z_{ur}(t)] - c_{sr}[\dot{z}_{sr}(t) - \dot{z}_{ur}(t)]\},
\end{aligned} \tag{4}$$

where

$$a_1 = \frac{1}{m_s} + \frac{l_1^2}{I_\varphi}, \quad a_2 = \frac{1}{m_s} - \frac{l_1l_2}{I_\varphi}, \; a_3 = \frac{1}{m_s} + \frac{l_2^2}{I_\varphi}.$$

To express the state-space representation, we set up the states as shown in follow the Table 1: The dynamics (3)-(4) can be rewritten in the following state-space model:

$$\dot{x}(t) = Ax(t) + Bu(t) + Gw(t), \tag{5}$$

where

$$\begin{aligned}
x(t) &= \begin{bmatrix} x_1(t)\, x_2(t)\, x_3(t)\, x_4(t) \\ \times\; x_5(t)\, x_6(t)\, x_7(t)\, x_8(t) \end{bmatrix}^T, \\
u(t) &= [u_f(t)\, u_r(t)]^T, \\
A &= \begin{bmatrix} 0_{4\times4} & a_{12} \\ a_{21} & a_{22} \end{bmatrix}, \\
B &= \begin{bmatrix} 0 & 0 & 0 & 0 & a_1 & a_2 & -\frac{1}{m_{uf}} & 0 \\ 0 & 0 & 0 & 0 & a_2 & a_3 & 0 & -\frac{1}{m_{ur}} \end{bmatrix}, \\
G &= \begin{bmatrix} 0 & 0 & -1 & 0 & 0 & 0 & 0 & 0 \\ 0 & 0 & 0 & -1 & 0 & 0 & 0 & 0 \end{bmatrix}, \\
a_{12} &= \begin{bmatrix} 1 & 0 & -1 & 0 \\ 0 & 1 & 0 & -1 \\ 0 & 0 & 1 & 0 \\ 0 & 0 & 0 & 1 \end{bmatrix}, \\
a_{21} &= \begin{bmatrix} -a_1\, k_{sf} & -a_2\, k_{sr} & 0 & 0 \\ -a_2\, k_{sf} & -a_3\, k_{sr} & 0 & 0 \\ \frac{k_{sf}}{m_{uf}} & 0 & -\frac{k_{sf}}{m_{uf}} & 0 \\ 0 & \frac{k_{sr}}{m_{ur}} & 0 & -\frac{k_{sr}}{m_{ur}} \end{bmatrix}, \\
a_{22} &= \begin{bmatrix} -a_1\, c_{sf} & -a_2\, c_{sr} & a_1\, c_{sf} & a_2\, c_{sr} \\ -a_2\, c_{sf} & -a_3\, c_{sr} & a_2\, c_{sf} & a_3\, c_{sr} \\ \frac{c_{sf}}{m_{uf}} & 0 & -\frac{c_{sf}}{m_{uf}} & 0 \\ 0 & \frac{c_{sr}}{m_{ur}} & 0 & -\frac{c_{sr}}{m_{ur}} \end{bmatrix},
\end{aligned} \tag{6}$$

where $w(t) = [\dot{z}_{rf}(t)\ \dot{z}_{rr}(t)]^T$ is the disturbance input, and $0_{4\times4}$ is a 4×4 zero matrix. For the performance requirements of the suspension system, three important characteristics can be set as the controlled output. These requirements can be divided into two types: minimized and restricted. The first is ride comfort, which is a performance index that must be minimized and is primarily measured using body acceleration. The other performance indices must be limited: handling performance and suspension structure limitation

$$\begin{aligned}
\left|z_{sf}(t) - z_{uf}(t)\right| &\le z_{f,max}, \\
|z_{sr}(t) - z_{ur}(t)| &\le z_{r,max}, \\
\left|k_{sf}(z_{uf}(t) - z_{rf}(t))\right| &\le F_f, \\
|k_{sr}(z_{ur}(t) - z_{rr}(t))| &\le F_r.
\end{aligned}$$

These can be expressed as tire and suspension deflections, respectively. Considering the above performance indices, the two control outputs can be defined as follows:

$$\begin{aligned}
z_1(t) &= \begin{bmatrix} \ddot{z}_c(t) & \ddot{\varphi}(t) \end{bmatrix}^T, \\
z_2(t) &= \begin{bmatrix} z_{sf}(t) - z_{uf}(t) & z_{sr}(t) - z_{ur}(t) \\ \times & z_{uf}(t) - z_{rf}(t) & z_{ur}(t) - z_{rr}(t) \end{bmatrix}^T
\end{aligned} \tag{7}$$

Thus, the entire space model of a half-vehicle suspension can be expressed as

$$\begin{aligned}\dot{x}(t) &= Ax(t) + Bu(t) + Gw(t),\\ z_1(t) &= C_1x(t) + D_1u(t),\\ z_2(t) &= C_2x(t) + D_2u(t),\\ y(t) &= Cx(t) + Du(t),\end{aligned} \tag{8}$$

where A, B, and B_1 are denoted in (6), and

$$C_1 = \begin{bmatrix} -\frac{k_{sf}}{m_s} & -\frac{k_{sr}}{m_s} & 0 & 0 \\ \frac{l_1k_{sf}}{I_\varphi} & -\frac{l_2k_{sr}}{I_\varphi} & 0 & 0 \\ -\frac{c_{sf}}{m_s} & -\frac{c_{sr}}{m_s} & \frac{c_{sf}}{m_s} & \frac{c_{sr}}{m_s} \\ \frac{l_1c_{sf}}{I_\varphi} & -\frac{l_2c_{sr}}{I_\varphi} & -\frac{l_1c_{sf}}{I_\varphi} & \frac{l_2c_{sr}}{I_\varphi} \end{bmatrix},$$

$$D_1 = \begin{bmatrix} \frac{1}{m_s} & \frac{1}{m_s} \\ -\frac{l_1}{I_\varphi} & \frac{l_2}{I_\varphi} \end{bmatrix},$$

$$C_2 = \begin{bmatrix} \frac{1}{z_{f,max}} & 0 & 0 & 0 & 0 & 0 & 0 & 0 \\ 0 & \frac{1}{z_{r,max}} & 0 & 0 & 0 & 0 & 0 & 0 \\ 0 & 0 & \frac{k_{sf}}{F_f} & 0 & 0 & 0 & 0 & 0 \\ 0 & 0 & 0 & \frac{k_{sr}}{F_r} & 0 & 0 & 0 & 0 \end{bmatrix}. \tag{9}$$

Before constructing the entire model, including the actuator dynamics, the dynamics of the subsystems (fluid dynamics, servo valve, hydraulic cylinder, and load) that constitute the actuator should be understood. According to [8], the hydraulic actuator system includes a cylinder, servo valve, and load attached to the piston. The actuator is responsible for transmitting forces and motions to external loads or systems. The cylinder located between the sprung and unsprung masses was connected in parallel to the passive spring and damper. The dynamics of the actuator are as follows:

$$\begin{aligned}\dot{F}_i(t) &= -\beta F_i(t) - \alpha A_s^2(\dot{z}_{si}(t) - \dot{z}_{ui}(t))\\ &\quad + \gamma_a A_s\sqrt{P_s - \frac{\mathrm{sgn}(x_{vi}(t))F_i(t)}{A_s}}x_{vi}(t),\\ \dot{x}_{vi}(t) &= \frac{1}{\tau}(-x_{vi}(t) + K_v u_i(t)),\end{aligned} \tag{10}$$

where i is f or r; P_s and A_s represent the hydraulic supply pressure and the actuator ram area, respectively. The displacement of the spool valve is represented by $x_{vi}(t)$; $u_i(t)$ is the control input voltage to the servo valve. Additionally, $\alpha = 4\beta_e/V_t$, $\beta = \alpha C_{tm}$, and $\gamma_a = \alpha C_d\omega_a\sqrt{1/\rho_a}$, where β_e is the effective bulk modulus. The total volume of actuator is represented by V_t; C_{tm} represents the leakage coefficient due to pressure. The discharge coefficient and the spool valve area gradient are represented by C_d and ω_a, respectively; ρ_a is the hydraulic fluid density; τ is the time constant of the spool valve dynamics, and K_v is the conversion gain. The dynamics equation (10) of the actuator can be expressed in the following time-varying state-space model:

$$\dot{x}_c(t) = A_c(t)x_c(t) + B_cu_c(t) + \xi_cx(t), \tag{11}$$

where

$$\begin{aligned}x_c(t) &= \begin{bmatrix} F_f(t) & F_r(t) & x_{vf}(t) & x_{vr}(t) \end{bmatrix}^T,\\ u_c &= \begin{bmatrix} u_f(t) & u_r(t) \end{bmatrix}^T,\end{aligned} \tag{12}$$

$$A_c(t) = \begin{bmatrix} -\beta & 0 & \gamma A_s\delta_f(t) & 0 \\ 0 & -\beta & 0 & \gamma A_s\delta_r(t) \\ 0 & 0 & -\frac{1}{\tau} & 0 \\ 0 & 0 & 0 & -\frac{1}{\tau} \end{bmatrix},$$

$$B_c = \begin{bmatrix} 0 & 0 \\ 0 & 0 \\ \frac{K_c}{\tau} & 0 \\ 0 & \frac{K_c}{\tau} \end{bmatrix},$$

$$\xi_c = \left[\begin{array}{c|cccc} 0_{1\times4} & -\alpha A_s^2 & 0 & \alpha A_s^2 & 0 \\ 0_{1\times4} & 0 & -\alpha A_s^2 & 0 & \alpha A_s^2 \\ 0_{1\times4} & 0 & 0 & 0 & 0 \\ 0_{1\times4} & 0 & 0 & 0 & 0 \end{array}\right] \tag{13}$$

where $\delta_f(t) = \sqrt{P_s - \frac{\mathrm{sgn}(x_{vf}(t))F_f(t)}{A_s}}$, $\delta_r(t) = \sqrt{P_s - \frac{\mathrm{sgn}(x_{vr}(t))F_r(t)}{A_s}}$. By incorporating the actuator dynamics (10) with the vehicle model (8), we can obtain the entire suspension state-space model including the electro-hydraulic actuator as follows:

$$\begin{aligned}\dot{x}_a(t) &= A_a(t)x_a(t) + B_au(t) + G_aw(t),\\ z_1(t) &= C_{1a}x_a(t),\quad z_2(t) = C_{2a}x_a(t),\\ y(t) &= C_ax_a(t),\end{aligned} \tag{14}$$

where

$$\begin{aligned}x_a(t) &= \begin{bmatrix} x(t) & x_c(t) \end{bmatrix}^T,\\ A_a(t) &= \left[\begin{array}{cc|c} A & B & 0_{8\times2} \\ \hline \xi_c & & A_c(t) \end{array}\right],\\ B_a &= \begin{bmatrix} 0_{8\times2} \\ B_c \end{bmatrix},\quad G_a = \begin{bmatrix} G \\ 0_{4\times2} \end{bmatrix}\\ C_{1a} &= \begin{bmatrix} C_1 & D_1 & 0_{2\times2} \end{bmatrix},\\ C_{2a} &= \begin{bmatrix} C_2 & D_2 & 0_{4\times2} \end{bmatrix},\\ C &= \begin{bmatrix} C & D & 0_{3\times2} \end{bmatrix}.\end{aligned} \tag{15}$$

The above suspension model (14) not only effectively incorporates the electro-hydraulic actuator dynamics but also includes nonlinear behaviors. Thus, the T–S fuzzy modeling technique is introduced to design the state estimator of the nonlinear suspension model. Here, the concept of "sector nonlinearity" [16] is applied to describe the nonlinear suspension system as a T–S fuzzy model. In real applications, the forces $F_i(t)$ (where i denotes f and r, respectively) are bounded between $[F_{i,min}, F_{i,max}]$. Therefore, the nonlinear terms ($\delta_i(t)$) of the actuator forces are also limited between $[\delta_{i,min}, \delta_{i,max}]$. Thus, $\delta_i(t)$ can be expressed as

$$\delta_i = M_{1i}(\vartheta_i(t))\delta_{i,max} + M_{2i}(\vartheta_i(t))\delta_{i,min}, \tag{16}$$

where $\vartheta_i(t) = \delta_i(t)$ denotes a premise variable, and $M_{1i}(\vartheta_i(t))$ and $M_{2i}(\vartheta_i(t))$ denote the membership functions that can be obtained as follows:

$$\begin{aligned} M_{1i}(\vartheta_i(t)) &= \frac{\delta_i(t) - \delta_{i,min}}{\delta_{i,max} - \delta_{i,min}}, \\ M_{2i}(\vartheta_i(t)) &= \frac{\delta_{i,max} - \delta_i(t)}{\delta_{i,max} - \delta_{i,min}}, \end{aligned} \tag{17}$$

The membership functions $M_{1i}(\vartheta_i(t))$ and $M_{2i}(\vartheta_i(t))$ represent "high" and "low", respectively. Table 2 lists each fuzzy rule and its corresponding weighting functions. For notational simplicity, we denote $h(\vartheta(t))$ as $h(t)$. Based on this, we consider approximating the nonlinear hydraulic suspension systems (14) using the following T-S fuzzy models:

Plant Rule $\mathcal{R}^1$:
IF $\vartheta_f(t)$ is high, and $\vartheta_r(t)$ is high,
THEN $\dot{x_a}(t) = A_a^1 x_a(t) + B_a u(t) + G_a w(t)$,

where A_a^1 can be calculated by substituting δ_f with $\delta_{f,max}$ and δ_r with $\delta_{r,max}$, from $A_a(t)$ in (14).

Plant Rule $\mathcal{R}^2$:
IF $\vartheta_f(t)$ is high, and $\vartheta_r(t)$ is low,
THEN $\dot{x_a}(t) = A_a^2 x_a(t) + B_a u(t) + G_a w(t)$,

where A_a^2 can be calculated by substituting δ_f with $\delta_{f,max}$ and δ_r with $\delta_{r,min}$, from $A_a(t)$ in (14).

Plant Rule $\mathcal{R}^3$:
IF $\vartheta_f(t)$ is low, and $\vartheta_r(t)$ is high,
THEN $\dot{x_a}(t) = A_a^3 x_a(t) + B_a u(t) + G_a w(t)$,

where A_a^3 can be calculated by substituting δ_f with $\delta_{f,min}$ and δ_r with $\delta_{r,max}$, from $A_a(t)$ in (14).

Plant Rule $\mathcal{R}^4$:
IF $\vartheta_f(t)$ is low, and $\vartheta_r(t)$ is low,
THEN $\dot{x_a}(t) = A_a^4 x_a(t) + B_a u(t) + G_a w(t)$,

where A_a^4 can be calculated by substituting δ_f with $\delta_{f,min}$ and δ_r with $\delta_{r,min}$, from $A_a(t)$ in (14).

Thus, under the limit conditions $\delta_f(t) \in [\delta_{f,min},\ \delta_{f,max}]$ and $\delta_r(t) \in [\delta_{r,min},\ \delta_{r,max}]$ for the front and rear actuator forces, respectively, a suitable T-S fuzzy model, including the electro-hydraulic actuator dynamics, can be represented as

TABLE 2. Fuzzy rules and corresponding weight functions.

Rule	$\vartheta_f(t)$	$\vartheta_r(t)$	Fuzzy weight
1	high	high	$h_1(t) = M_{1f}(t) \times M_{1r}(t)$
2	high	low	$h_2(t) = M_{1f}(t) \times M_{2r}(t)$
3	low	high	$h_3(t) = M_{2f}(t) \times M_{1r}(t)$
4	low	low	$h_4(t) = M_{2f}(t) \times M_{2r}(t)$

$$\begin{aligned} \dot{x_a}(t) &= \sum_{i=1}^{4} h_i(t) A_a^i x_a(t) + B_a u(t) + G_a w(t), \\ z_1(t) &= C_{1a}\bar{x}(t), \quad z_2(t) = C_{2a} x_a(t), \\ y(t) &= C_a x_a(t), \end{aligned} \tag{18}$$

where $h_i(\vartheta(t))$ satisfies $h_i(\vartheta(t)) \geq 0$ and $\sum_{i=1}^{4} h_i(\vartheta(t)) = 1$. We employ $h_i(\vartheta(t)) = h_i$ for the convenience of notation. In practice, $F_i(t)$ and the spool valve position ($x_{vi}(t)$) are measurable values; thus, the proposed fuzzy system (18) can be implemented in practice.

In most control engineering problems, controllers or state estimators are implemented using digital computers. Because the continuous time measurements captured by the sensor are sampled and quantized to be converted into a discrete signal, a discrete time state estimation technique must be considered. If T_s is the sampling time of the micro control unit (MCU), we can easily convert a discrete-time system to a continuous-time system (18) using the zero-order hold (ZOH) method as follows:

$$\left(\begin{array}{c|cc} \bar{A}_d^i & \bar{G}_d & \bar{B}_d \\ \hline \bar{C}_d & 0_{3\times2} & 0_{3\times2} \\ \bar{C}_{1d} & 0_{4\times2} & 0_{4\times2} \\ \bar{C}_{2d} & 0_{2\times2} & 0_{2\times2} \end{array}\right) = \left(\begin{array}{c|cc} \bar{A}^i & \bar{G} & \bar{B} \\ \hline \bar{C} & 0_{3\times2} & 0_{3\times2} \\ \bar{C}_1 & 0_{4\times2} & 0_{4\times2} \\ \bar{C}_2 & 0_{2\times2} & 0_{2\times2} \end{array}\right). \tag{19}$$

The newly obtained discrete-time counterparts of the T-S fuzzy models are represented as follows:

$$\begin{aligned} x_{k+1} &= A_k x_k + B_k u_k + G_k w_k, \\ y_k &= C_k x_k + v_k, \\ z_{1k} &= C_{1k} x_k, \\ z_{2k} &= C_{2k} x_k, \end{aligned} \tag{20}$$

where A_k, B_k, C_k, and G_k are defined as

$$\begin{aligned} A_k &\triangleq \sum_{i=1}^{4} h_i(\vartheta_k) A_d^i, \quad B_k \triangleq \sum_{i=1}^{4} h_i(\vartheta_k) B_d^i, \\ C_k &\triangleq \sum_{i=1}^{4} h_i(\vartheta_k) C_d^i, \quad G_k \triangleq \sum_{i=1}^{4} h_i(\vartheta_k) G_d^i. \end{aligned} \tag{21}$$

where k denotes the samples of time kT_s with a sampling period of T_s.

III. FUZZY FINITE MEMORY(FFM) ESTIMATOR FOR ACTIVE SUSPENSION SYSTEMS

From the discrete-time T-S fuzzy model (20), the stacked input and measurement U_{k-1} and Y_{k-1} can be represented by

$$\begin{aligned} U_{k-1} &= [u_{k-N}^T, u_{k-N+1}^T, \ldots, u_{k-1}^T]^T, \\ Y_{k-1} &= [y_{k-N}^T, y_{k-N+1}^T, \ldots, y_{k-1}^T]^T, \\ &= \bar{C}_N(k)x_{k-N} + \bar{B}_N(k)U_{k-1} \\ &\quad + \bar{G}_N(k)W_{k-1} + V_{k-1}, \end{aligned} \tag{22}$$

where N denotes the horizon size, which is the number of most recently used inputs and measurements, and the matrices and stacked noise vectors $\bar{C}_N(k)$, $\bar{B}_N(k)$, $\bar{G}_N(k)$, W_{k-1}, and V_{k-1} are expressed as follows:

$$\bar{C}_N(k) = \begin{bmatrix} C_{k-N} \\ C_{k-N+1}\mathcal{A}_{k-N}^{k-N} \\ C_{k-N+2}\mathcal{A}_{k-N+1}^{k-N} \\ \vdots \\ C_{k-1}\mathcal{A}_{k-2}^{k-N} \end{bmatrix}$$

$$\bar{B}_N(k) = \begin{bmatrix} 0 & 0 \\ C_{k-N+1}B_{k-N} & 0 \\ C_{k-N+2}\mathcal{A}_{k-N+1}^{k-N+1}B_{k-N} & C_{k-N+2}B_{k-N+1}, \\ \vdots & \vdots \\ C_{k-1}\mathcal{A}_{k-2}^{k-N-1}B_{k-N} & C_{k-1}\mathcal{A}_{k-2}^{k-N+2}B_{k-N+1} \end{bmatrix}$$

$$\begin{bmatrix} \cdots & 0 & 0 \\ \cdots & 0 & 0 \\ \cdots & 0 & 0 \\ \cdots & \ddots & \vdots \\ \cdots & C_{k-1}B_{k-2} & 0 \end{bmatrix},$$

$$\bar{G}_N(k) = \begin{bmatrix} 0 & 0 \\ C_{k-N+1}G_{k-N} & 0 \\ C_{k-N+2}\mathcal{A}_{k-N+1}^{k-N+1}G_{k-N} & C_{k-N+2}G_{k-N+1}, \\ \vdots & \vdots \\ C_{k-1}\mathcal{A}_{k-2}^{k-N-1}G_{k-N} & C_{k-1}\mathcal{A}_{k-2}^{k-N+2}G_{k-N+1} \end{bmatrix}$$

$$\begin{bmatrix} \cdots & 0 & 0 \\ \cdots & 0 & 0 \\ \cdots & 0 & 0 \\ \cdots & \ddots & \vdots \\ \cdots & C_{k-1}G_{k-2} & 0 \end{bmatrix},$$

$$\begin{aligned} W_{k-1} &= [w_{k-N}^T, w_{k-N+1}^T, \ldots, w_{k-1}^T]^T, \\ V_{k-1} &= [v_{k-N}^T, v_{k-N+1}^T, \ldots, v_{k-1}^T]^T. \end{aligned}$$

The fuzzy finite memory (FFM) estimator can be expressed as follows:

$$\hat{x}_k = H_{k-1}Y_{k-1} + L_{k-1}U_{k-1}, \tag{23}$$

where $\hat{x}_k$ is the estimated state in the time sequence k and H_{k-1} and L_{k-1} denote the gain matrices of the FFM estimator. The estimated state $\hat{x}_k$ can be expressed using the stacked measurement vector (22) as follows:

$$\begin{aligned} \hat{x}_k = H_{k-1}(&\bar{C}_N(k)x_{k-N} + \bar{B}_N(k)U_{k-1} + \bar{G}_N(k)W_{k-1} \\ &+ V_{k-1}) + L_{k-1}U_{k-1}. \end{aligned} \tag{24}$$

Introduce the relation between x_k and x_{k-N} as follows:

$$x_k = A_{k-1}^{k-N}x_{k-N} + F_u(k)U_{k-1} + F_w(k)W_{k-1}, \tag{25}$$

where

$$\begin{aligned} F_u(k) = \Big[&\mathcal{A}_{k-1}^{k-N} \quad \mathcal{A}_{k-1}^{k-N+1}B_{k-N} \\ &\cdots \quad \mathcal{A}_{k-1}^{k-1}B_{k-2}\ B_{k-1}\Big], \end{aligned} \tag{26}$$

$$\begin{aligned} F_w(k) = \Big[&\mathcal{A}_{k-1}^{k-N} \quad \mathcal{A}_{k-1}^{k-N+1}G_{k-N} \\ &\cdots \quad \mathcal{A}_{k-1}^{k-1}G_{k-2}\ G_{k-1}\Big], \end{aligned} \tag{27}$$

$$\begin{aligned} \mathcal{A}_a^b &= \prod_{i=a}^{b} A_i, \\ \mathcal{A}_a^a &= A_a. \end{aligned} \tag{28}$$

Adding the zero term (25) into the right-hand sides of (24) and taking the expectation on both sides yield:

$$\begin{aligned} \hat{x}_k = &E[\{H_{k-1}\bar{C}_N - A_{k-1}^{k-N}\}x_{k-N}] + E[x_k] \\ &+ E[\{L_{k-1} + H_{k-1}\bar{B}_N(k) - F_u(k)\}U_{k-1}]. \end{aligned} \tag{29}$$

The unbiased condition $E[x_k] = E[\hat{x}_k]$, should be satisfied. Thus, the following constraint must be ensured:

$$H_{k-1}\bar{C}_N = A_{k-1}^{k-N}, \tag{30}$$

$$L_{k-1} = -H_{k-1}\bar{B}_N(k) + F_u(k), . \tag{31}$$

In this study, we focus on the gain matrix H_{k-1} because L_{k-1} can be obtained if H_{k-1} is determined. With an accurate state estimate for the FFM estimator, the following theorem determines the FFM estimator gain H_{k-1}:

Theorem 1: The FFM estimator gain should satisfy the unbiased condition (30), and the gain is given by

$$H_{k-1} = \mathcal{A}_{k-1}^{k-N}(\bar{C}_N(k)^T\Omega_N^{-2}\bar{C}_N(k))^{-1}\bar{C}_N(k)^T\Omega_N^{-2}. \tag{32}$$

where $\Omega_N = diag(\omega^N I,\ \omega^{N-1}I, \ldots, \omega I)$ denotes the weight matrix with the weight parameter $0 \le \omega \le 1$, which gives more weight to recent data but less weight to old data.

Proof: Let $J = \|H_{k-1}\|_F^2$ be a cost function, where $\|\cdot\|_F$ denotes the Frobenius norm, then the minimum length solution in (30) can be obtained. We introduce the Lagrangian multiplier method with the Lagrange multiplier Γ to derive the minimum length solution of the FFM estimator gain H as follows:

$$\mathcal{L} = J + \Gamma(H_{k-1}\bar{C}_N(k) - \mathcal{A}_{k-1}^{k-N}), \tag{33}$$

To minimize (33), a partial derivative with respect to H_{k-1} is given as follows:

$$\frac{\partial \mathcal{L}}{\partial H_{k-1}} = 2H_{k-1}\Omega_N^2 + \Gamma\bar{C}_N(k)^T = 0 \tag{34}$$

yields

$$H_{k-1} = -0.5\Gamma \bar{C}_N(k)^T \Omega_N^{-2} \tag{35}$$

Substituting (35) into (30) yields

$$-0.5\Gamma \tilde{C}_N(k)^T \Omega_N^{-2} \bar{C}_N(k) = \mathcal{A}_{k-1}^{k-N} \tag{36}$$

which provides

$$\Gamma = -2\mathcal{A}_{k-1}^{k-N} (\bar{C}_N(k)^T \Omega_N^{-2} \bar{C}_N(k))^{-1} \tag{37}$$

Finally, the estimator gain H_{k-1} can be obtained by substituting (37) into (35) as follows:

$$H_{k-1} = \mathcal{A}_{k-1}^{k-N} (\bar{C}_N(k)^T \Omega_N^{-2} \bar{C}_N(k))^{-1} \bar{C}_N(k)^T \Omega_N^{-2}, \tag{38}$$

which completes the proof. □

The FFM estimator can be summarized with the following remark.

Remark 1: The FFM estimation can be represented by substituting (31) into (23) as follows:

$$\hat{x}_k = H_{k-1} Y_{k-1} - [H_{k-1} \bar{B}_N(k) + F_u(k)] U_{k-1}, \tag{39}$$

where the estimator gain H_{k-1} is represented in (38).

The proposed FFM estimator approximates a complex nonlinear half-vehicle suspension model through T-S fuzzy modeling and is designed based on a finite memory structure, which uses only recent N inputs and measurements. Infinite memory structures, such as the Kalman filter, accumulate errors because they use past estimates, whereas the FFM estimator has a finite memory structure, and thus, errors do not accumulate.

Remark 2: The minimum length solution to obtain the gain matrix H_{k-1} enhances the robustness by reducing the effects of uncertainties [36]. The stacked measurement (22) can be represented by $Y_{k-1} = Y_{k-1}^r + Y_{k-1}^u$, where Y_{k-1}^r and Y_{k-1}^u are real and uncertain measurements, respectively. The estimated state (23) can be represented as:

$$\begin{aligned} \hat{x}_k &= H_{k-1} Y_{k-1} + L_{k-1} U_{k-1} \\ &= H_{k-1} Y_{k-1}^r + H_{k-1} Y_{k-1}^u + L_{k-1} U_{k-1}, \end{aligned} \tag{40}$$

where $H_{k-1} Y_{k-1}^r$ and $H_{k-1} Y_{k-1}^u$ denote the real estimated state and uncertain estimate, respectively. Taking a Frobenius norm on both sides of (40) yields:

$$\begin{aligned} \|\hat{x}_k\|_F &= \|H_{k-1} Y_{k-1}^r + H_{k-1} Y_{k-1}^u + L_{k-1} U_{k-1}\|_F \\ &\le \|H_{k-1} Y_{k-1}^r\|_F + \|H_{k-1} Y_{k-1}^u\|_F + \|L_{k-1} U_{k-1}\|_F. \end{aligned} \tag{41}$$

The uncertain estimates $H_{k-1} Y_{k-1}^u$ can be reduced when H_{k-1} is the minimum length solution.

Remark 3: For state estimation, the extended state observer (ESO) is widely used owing to its advantage in that both the states and model uncertainties can be estimated [39], [40]. Although the extended state observer also has the limitation of having an IIR structure; therefore, a comparison with the finite memory state estimator would be an interesting topic for our future research.

TABLE 3. Parameters for the half-vehicle.

Parameter	m_s	m_{uf}	m_{ur}	I_φt
Unit	kg	kg	kg	kgm^2
Value	690	40	45	1222
Parameter	k_{sf}	k_{sr}	k_{tf}	k_{tr}
Unit	N/m	N/m	N/m	N/m
Value	18000	22000	200000	200000
Parameter	c_{sf}	c_{sr}	l_1	l_2
Unit	Ns/m	Ns/m	m	m
Value	1000	1000	1.3	1.5

TABLE 4. Parameters for the hydraulic actuator.

Parameter	P_s	A_s
Unit	Pa	m^2
Value	10343500	3.35×10^{-4}
Parameter	τ	K_v
Unit	s	m/V
Value	0.003	0.001
Parameter	α	β
Unit	N/m^5	s^{-1}
Value	4.515×10^{13}	1
Parameter	γ	
Unit	N/m$^{5/2}$/kg$^{1/2}$	
Value	1.545×10^9	

IV. SIMULATION RESULTS

In this section, we present the simulation results for the state estimation performance of the proposed FFM estimator for a nonlinear hydraulic suspension system. The parameters for the half-vehicle suspension are listed in Table 3, and the parameters for each actuator are listed in Table 4. To effectively evaluate the suspension performance, it is necessary to consider the variability of the road profile in the context of comfortable riding, steering, and physical specifications. In this simulation, two different road profiles were considered to evaluate the performance of the proposed state estimator.

A. BUMP RESPONSE

First, we considered the time responses for the isolated bump road profiles. The corresponding disturbance can be expressed as:

$$z_r(t) = \begin{cases} \dfrac{H}{2}\left(1 - \cos\left(\dfrac{2\pi V}{L} t\right)\right), & \text{if } 0 \le t \le \dfrac{L}{V}, \\ 0, & \text{if } t > \dfrac{L}{V}, \end{cases} \tag{42}$$

In this case, we set the height of the bump to $H = 50$ mm, the length of the bump as $L = 6$ m, and the vehicle forward velocity as $V = 35$ km/h. In addition, it was assumed that the road profile of the rear wheel $z_{rr}(t)$ has a time delay of approximately $(l_1 + l_2)/V$ compared to that of the front wheel. The initial state of the estimator is set as the zero-initial condition. The noise covariances of the external

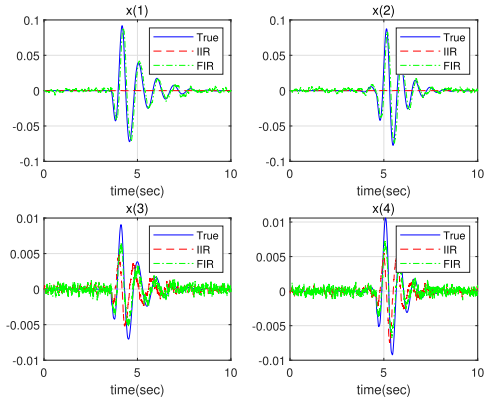

FIGURE 2. True state and its estimation using the fuzzy KF and FFN estimator.

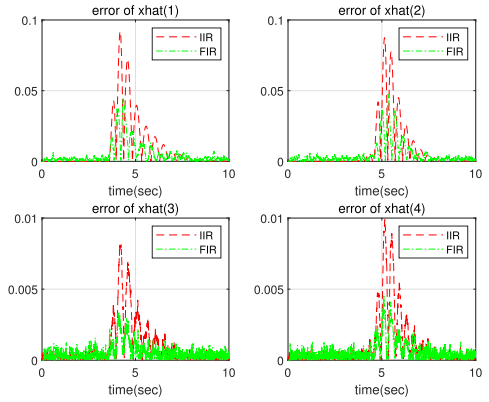

FIGURE 3. Estimator errors of two estimators concerning the front/rear suspension deflection and tire deflection.

disturbance w_k are taken as $Q_k = (H/2)((2\pi V)/L))^2\ I$. The sensor noise v_k is assumed to be a normal distribution $\mathcal{N}(0.01^2, 0.01^2, 0.001^2, 0.001^2)$. The length of the finite memory horizon, which is a design parameter, was taken as $N = 50$. Figure 2 shows the true states $(x_1(t) \sim x_4(t))$ and their estimations $\hat{x}_1(t) \sim \hat{x}_4(t)$ using a fuzzy KF and an FFM estimator for the front/rear suspension deflection and tire deflection, respectively. Figure 3 shows the estimation errors of two estimators for the state values. As shown in Figures 2 and 3, the fuzzy KF exhibited a large estimation error in the external disturbance period. However, the proposed FFM estimator exhibited a smaller estimation error than the fuzzy KF owing to its characteristic finite memory structure. These results verified that the proposed FFM estimator is more robust against external disturbance than the fuzzy KF is. To further demonstrate the performance of the proposed estimator, we evaluated the estimator performance in the presence of modeling uncertainties. A modeling uncertainty matrix, denoted as ΔA_k was set as:

$$\Delta A_k = \begin{cases} 0.01I & 5(L/V) \le k \le 7(L/V), \\ 0, & \text{otherwise}, \end{cases} \tag{43}$$

Figure 4 shows the true states $(x_1(t) \sim x_4(t))$ and their estimations $(\hat{x}_1(t) \sim \hat{x}_4(t))$ using the fuzzy KF and FFN estimators for the front/rear suspension deflection and tire deflection, respectively. Figure 5 shows the estimator errors

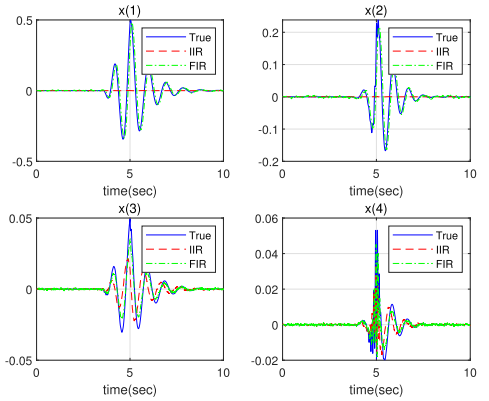

FIGURE 4. True state and its estimation using the fuzzy KF and FFN estimator.

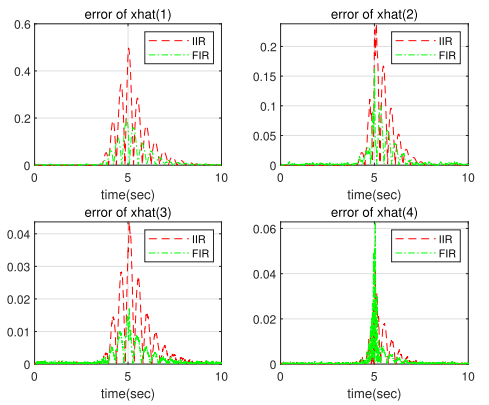

FIGURE 5. Estimator errors of the two estimators for the front/rear suspension deflection and tire deflection.

of the two estimators for the state values. As shown in the above simulations, a significant increase in the estimation error occurred when modeling uncertainties are present. The fuzzy KF exhibited dramatic increases in the estimation errors in the presence of modeling uncertainties. However, the estimation error of the proposed FFM is much smaller than that of the fuzzy KF. These results show that the proposed FFM estimator have more robust performance against the modeling uncertainty than the fuzzy KF. Similar results were also demonstrated in the following rough road profile.

B. ROUGH ROAD RESPONSE

In this simulation, we considered the following rough road condition:

$$z_r(t) = 0.0254\sin(2\pi t) + 0.005\sin(10.5\pi t) + 0.001\sin(21.5\pi t)(\text{m}). \tag{44}$$

According to [16], Equation (25) effectively describes rough road surfaces. It is assumed that the road disturbance is similar to the vehicle body resonance frequency (1 Hz) with a high-frequency disturbance.

Figure 6 shows the responses of the true states $(x_1(t) \sim x_4(t))$ and their estimations $(\hat{x}_1(t) \sim \hat{x}_4(t))$. Figure 7 shows the estimation errors of the two estimators for the front/rear suspension deflection and tire deflection, respectively. As shown in Figures 6 and 7, the proposed FFM

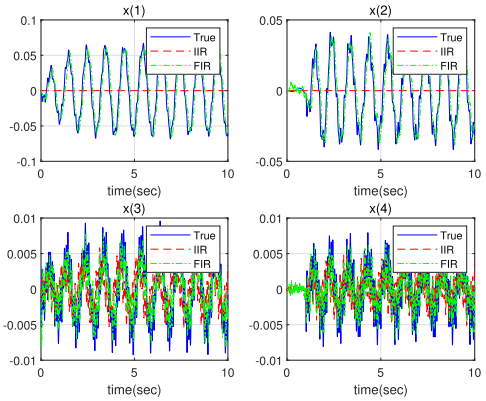

FIGURE 6. True state and its estimation using the fuzzy KF and FFN estimators.

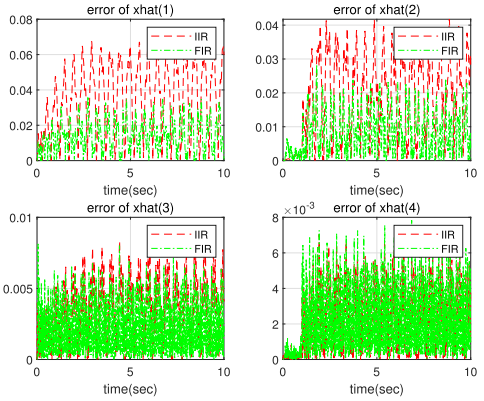

FIGURE 7. Estimator errors of the two estimators for the front/rear suspension deflection and tire deflection.

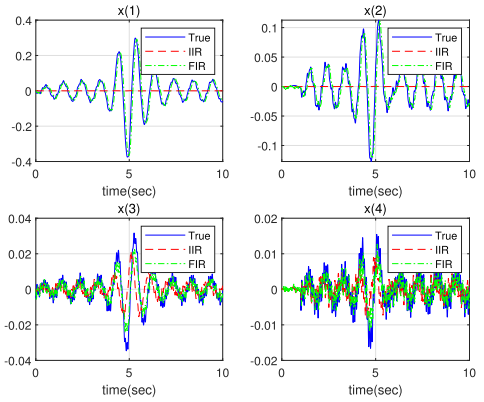

FIGURE 8. True state and its estimation using the fuzzy KF and FFN estimator.

estimator has significantly fewer estimation errors than the IIR structure (fuzzy KF) in the external disturbances period. These results verify that the proposed FFM estimator is more robust against external disturbances than the fuzzy KF. All the results shown above are due to the characteristic finite memory structure of the proposed estimator. As with the bump disturbances, we also evaluated the estimate performance when modeling uncertainties in the rough road conditions. Figure 8 represents the responses of true states ($x_1(t) \sim x_4(t)$) and their estimations ($\hat{x}_1(t) \sim \hat{x}_4(t)$). Figure 9 represents the estimation errors of the two estimators for the fron/rear

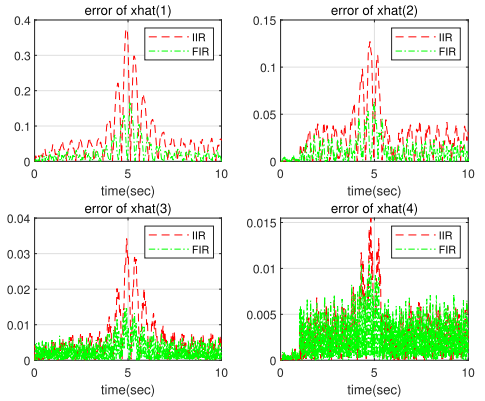

FIGURE 9. Estimator errors of the two estimators for the front/rear suspension deflection and tire deflection.

suspension deflection and tire deflection, respectively. In case of the Kalman filter, a dramatic increase in the estimation error occurs where modeling errors exist. However, the FFM estimator produces much smaller estimation errors than the fuzzy KF estimator. These results also show that the performance of the proposed estimator is robust under temporary modeling uncertainty owing to its finite memory structure.

V. CONCLUSION

In this paper, we present a new nonlinear state estimator with a finite memory structure for active suspension systems. By using the concept of ''sector nonlinearity,'' a half-vehicle with two electro-hydraulic actuators was effectively expressed using a T–S fuzzy model. A batch-form FFM estimator for a linear discrete time-varying system was designed and applied to a nonlinear suspension system described as a fuzzy model. Compared with the conventional state estimator, which is known to have an infinite memory structure and requires whole data from the initial time to the current time to operate, the proposed state estimator has a finite memory structure and guarantees robustness to unknown initial data. Simulation results are presented to illustrate the estimation performance and robustness of the finite memory estimator for highly nonlinear suspension systems. Compared with the conventional IIR-based state estimator, the presented FFM estimator exhibits excellent robustness performance when external disturbances and temporary model uncertainty exist. Therefore, estimators with finite memory structures are expected to be good alternatives for several control engineering applications.

REFERENCES

[1] J. Cao, H. Liu, P. Li, and D. J. Brown, ''State of the art in vehicle active suspension adaptive control systems based on intelligent methodologies,'' *IEEE Trans. Intell. Transp. Syst.*, vol. 9, no. 3, pp. 392–405, Sep. 2008.

[2] H. Chen and K. Guo, ''Constrained H_∞ control of active suspensions: An LMI approach,'' *IEEE Trans. Control Syst. Technol.*, vol. 13, no. 3, pp. 412–421, May 2005.

[3] H. Du and N. Zhang, ''H_∞ control of active vehicle suspensions with actuator time delay,'' *J. Sound Vib.*, vol. 301, nos. 1–2, pp. 236–252, Mar. 2007.

[4] D. Hrovat, ''Survey of advanced suspension developments and related optimal control applications,'' *Automatica*, vol. 33, no. 10, pp. 1781–1817, 1997.

[5] R. A. Williams, "Automotive active suspensions part 2: Practical considerations," *Proc. Inst. Mech. Eng., D, J. Automobile Eng.*, vol. 211, no. 6, pp. 427–444. Jun. 1997.

[6] M. Yamashita, K. Fujimori, K. Hayakawa, and H. Kimura, "Application of H_∞ control to active suspension systems," *IFAC Proc. Vols.*, vol. 26, no. 2, pp. 87–90, 1993.

[7] H. Gao, W. Sun, and P. Shi, "Robust sampled-data H_∞ control for vehicle active suspension systems," *IEEE Trans. Control Syst. Technol.*, vol. 18, no. 1, pp. 238–245, Jan. 2010.

[8] H. D. Choi, C. K. Ahn, M. T. Lim, and M. K. Song, "Dynamic output feedback H_∞ control for active half-vehicle suspension systems with time-varying input delay," *Int. J. Control, Autom. Syst.*, vol. 14, no. 1, pp. 59–68, 2015.

[9] P. C. Chen and A. C. Huang, "Adaptive sliding control of active suspension systems with uncertain hydraulic actuator dynamics," *Vehicle Syst. Dyn.*, vol. 44, no. 5, pp. 268–357, May 2006.

[10] H. Du and N. Zhang, "Fuzzy control for nonlinear uncertain electrohydraulic active suspensions with input constraint," *IEEE Trans. Fuzzy Syst.*, vol. 17, no. 2, pp. 343–356, Apr. 2009.

[11] H. Du and N. Zhang, "Takagi-Sugeno fuzzy control scheme for electrohydraulic active suspensions," *Control Cybern.*, vol. 39, no. 4, pp. 1095–1115, 2010.

[12] S. Bououden, M. Chadli, and H. R. Karimi, "A robust predictive control design for nonlinear active suspension systems," *Asian J. Control*, vol. 18, no. 1, pp. 122–132, Jan. 2016.

[13] T. Gao, J. Yang, L. Jia, Y. Deng, W. Zhang, and Z. Zhang, "Design of new energy-efficient permanent magnetic maglev vehicle suspension system," *IEEE Access*, vol. 7, pp. 135917–135932, 2019.

[14] D. Wang, D. Zhao, M. Gong, and B. Yang, "Research on robust model predictive control for electro-hydraulic servo active suspension systems," *IEEE Access*, vol. 6, pp. 3231–3240, 2018.

[15] S. Liu, R. Hao, D. Zhao, and Z. Tian, "Adaptive dynamic surface control for active suspension with electro-hydraulic actuator parameter uncertainty and external disturbance," *IEEE Access*, vol. 8, pp. 156645–156653, 2020.

[16] H. D. Choi, C. J. Lee, and M. T. Lim, "Fuzzy preview control for half-vehicle electro-hydraulic suspension system," *Int. J. Control, Autom. Syst.*, vol. 16, no. 5, pp. 2489–2500, Oct. 2018.

[17] T. Takagi and M. Sugeno, "Fuzzy identification of systems and its applications to modeling and control," *IEEE Trans. Syst., Man, Cybern.*, vol. SMC-15, no. 1, pp. 116–132, Jan. 1985.

[18] H. Li, H. Liu, H. Gao, and P. Shi, "Reliable fuzzy control for active suspension systems with actuator delay and fault," *IEEE Trans. Fuzzy Syst.*, vol. 20, no. 2, pp. 342–357, Apr. 2012.

[19] H. D. Choi, C. K. Ahn, P. Shi, L. Wu, and M. T. Lim, "Dynamic output-feedback dissipative control for T–S fuzzy systems with time-varying input delay and output constraints," *IEEE Trans. Fuzzy Syst.*, vol. 25, no. 3, pp. 511–526, Jun. 2017.

[20] G.-T. Ran, Z.-D. Lu, F.-X. Xu, and J.-X. Lu, "Event-triggered dynamic output feedback control for networked T-S fuzzy systems with asynchronous premise variables," *IEEE Access*, vol. 6, pp. 78740–78750, 2018.

[21] J. Shi and Q. Zhang, "Dynamic sliding-mode control for T-S fuzzy singular time-delay systems with H_∞ performance," *IEEE Access*, vol. 7, pp. 115388–115399, 2019.

[22] Z. Gao, X. Shi, and S. X. Ding, "Fuzzy state/disturbance observer design for T–S fuzzy systems with application to sensor fault estimation," *IEEE Trans. Syst., Man, Cybern., B, Cybern.*, vol. 38, no. 3, pp. 875–880, Jun. 2008.

[23] Q. Zhang, R. Li, and J. Ren, "Robust adaptive sliding mode observer design for T-S fuzzy descriptor systems with time-varying delay," *IEEE Access*, vol. 6, pp. 46002–46018, 2018.

[24] Z. Wang, Y. Qin, C. Hu, M. Dong, and F. Li, "Fuzzy observer-based prescribed performance control of vehicle roll behavior via controllable damper," *IEEE Access*, vol. 7, pp. 19471–19487, 2019.

[25] Y. E. Kim, H. H. Kang, and C. K. Ahn, "Two-layer nonlinear FIR filter and unscented Kalman filter fusion with application to mobile robot localization," *IEEE Access*, vol. 8, pp. 87173–87183, 2020.

[26] V. N. Giap, S.-C. Huang, Q. D. Nguyen, and T.-J. Su, "Disturbance observer-based linear matrix inequality for the synchronization of Takagi-Sugeno fuzzy chaotic systems," *IEEE Access*, vol. 8, pp. 225805–225821, 2020.

[27] H. Pan, W. Sun, H. Gao, T. Hayat, and F. Alsaadi, "Nonlinear tracking control based on extended state observer for vehicle active suspensions with performance constraints," *Mechatronics*, vol. 30, pp. 363–370, Sep. 2015.

[28] Z. Wang, M. Dong, Y. Qin, Y. Du, F. Zhao, and L. Gu, "Suspension system state estimation using adaptive Kalman filtering based on road classification," *Vehicle Syst. Dyn.*, vol. 55, no. 3, pp. 371–398, Mar. 2017.

[29] J. Na, Y. Huang, X. Wu, G. Gao, G. Herrmann, and J. Z. Jiang, "Active adaptive estimation and control for vehicle suspensions with prescribed performance," *IEEE Trans. Control Syst. Technol.*, vol. 26, no. 6, pp. 2063–2077, Nov. 2018.

[30] S. You, K. Kim, J. Moon, and W. Kim, "Extended state observer based robust position tracking control using nonlinear damping gain for quadrotors with external disturbance," *IEEE Access*, vol. 8, pp. 174558–174567, 2020.

[31] W. Kwon and O. Kwon, "FIR filters and recursive forms for continuous time-invariant state-space models," *IEEE Trans. Autom. Control*, vol. AC-32, no. 4, pp. 352–356, Apr. 1987.

[32] C. K. Ahn, S. Han, and W. H. Kwon, "H_∞ finite memory controls for linear discrete-time state-space models," *IEEE Trans. Circuits Syst. II, Exp. Briefs*, vol. 54, no. 2, pp. 97–101, Feb. 2007.

[33] S. Zhao, Y. S. Shmaliy, B. Huang, and F. Liu, "Minimum variance unbiased FIR filter for discrete time-variant systems," *Automatica*, vol. 53, pp. 355–361, Mar. 2015.

[34] C. K. Ahn, Y. S. Shmaliy, and S. Zhao, "A new unbiased FIR filter with improved robustness based on frobenius norm with exponential weight," *IEEE Trans. Circuits Syst. II, Exp. Briefs*, vol. 65, no. 4, pp. 521–525, Apr. 2018.

[35] C. K. Ahn and Y. S. Shmaliy, "New receding horizon FIR estimator for blind smart sensing of velocity via position measurements," *IEEE Trans. Circuits Syst. II, Exp. Briefs*, vol. 65, no. 1, pp. 135–139, Jan. 2018.

[36] S. H. You, C. K. Ahn, Y. S. Shmaliy, and S. Zhao, "Minimum weighted frobenius norm discrete-time FIR filter with embedded unbiasedness," *IEEE Trans. Circuits Syst. II, Exp. Briefs*, vol. 65, no. 9, pp. 1284–1288, Sep. 2018.

[37] Y. S. Shmaliy and O. Ibarra-Manzano, "Optimal finite impulse response estimation of linear models in receiver channels with imbedded digital signal processing units," *IET Signal Process.*, vol. 6, no. 4, pp. 281–287, Jun. 2012.

[38] Y. S. Shmaliy, "Linear optimal FIR estimation of discrete time-invariant state-space models," *IEEE Trans. Signal Process.*, vol. 58, no. 6, pp. 3086–3096, Jun. 2010.

[39] W. Deng, J. Yao, Y. Wang, X. Yang, and J. Chen, "Output feedback backstepping control of hydraulic actuators with valve dynamics compensation," *Mech. Syst. Signal Process.*, vol. 158, Sep. 2021, Art. no. 107769.

[40] W. Deng and J. Yao, "Extended-state-observer-based adaptive control of electrohydraulic servomechanisms without velocity measurement," *IEEE/ASME Trans. Mechatronics*, vol. 25, no. 3, pp. 1151–1161, Jun. 2020.

HYUN DUCK CHOI received the B.S. and integrated M.S./Ph.D. degrees in electrical engineering from Korea University, Seoul, South Korea, in 2011 and 2017, respectively. He was a Senior Research Engineer with Hyundai Mobis, Yongin, South Korea, and Samsung Electronics, Suwon, South Korea. He is currently an Assistant Professor with the School of Electronics and Computer Engineering, Chonnam National University, Gwangju, South Korea. His current research interests include robust control, estimation, fuzzy systems, neural networks, nonlinear systems, and their application to vehicle suspension systems.

SUNG HYUN YOU received the B.S. degree in electrical engineering from the Seoul National University of Science and Technology, Seoul, South Korea, in 2013, and the Ph.D. degree from the School of Electrical Engineering, Korea University, Seoul, in 2019. He was a Research Professor with the Research Institute of Engineering and Technology, Korea University. Since 2020, he has been an Assistant Professor with Chosun University, South Korea. His research interests include optimal, robust, intelligent, and receding horizon control and estimation.